

# Investigation on the Particle Growth of Rutile TiO<sub>2</sub> Suppressed by Manganese

Aripin<sup>1</sup>, Edvin Priatna<sup>1</sup>, Nundang Busaeri<sup>1</sup>, Rudi Priyadi<sup>2</sup>, I Nyoman Sudiana<sup>3</sup>, I Made Joni<sup>4</sup>, Svilen Sabchevski<sup>5</sup>

<sup>1</sup>Department of Electrical Engineering, Faculty of Engineering, Siliwangi University, Jl. Siliwangi 24, Tasikmalaya 46115, Indonesia

<sup>2</sup>Department of Agrotechnology, Faculty of Agriculture, Siliwangi University, Jl. Siliwangi 24, Tasikmalaya 46115, Indonesia

<sup>3</sup>Department of Physics, Faculty of Mathematics and Natural Sciences, University of Haluoleo, Kendari, Southeast Sulawesi 93132, Indonesia

<sup>4</sup>Nano Technology and Graphene Research Center (NTGRC), Padjadjaran University, Bandung, West Java 45363, Indonesia

<sup>5</sup>Lab. Plasma Physics and Engineering, Institute of Electronics of the Bulgarian Academy of Sciences, 72 Tzarigradsko Shose Blvd., Sofia 1784, Bulgaria

**Abstract.** In this paper, we present the results of an investigation on the crystallite growth of rutile TiO<sub>2</sub> and the formation of Mn–O–Ti bonds in a TiO<sub>2</sub>/manganese composition. The effects of manganese loading from 20 wt% to 80 wt%, into TiO<sub>2</sub> at a temperature of 1200°C on the structural properties, have been studied. The material's properties have been characterized on the basis of the experimental data obtained using X-ray diffraction (XRD), Fourier transform infrared (FTIR) spectroscopy and Scanning Electron Microscopy (SEM). It has been found that an increase of the loading by manganese up to 80 wt% leads to a decrease of the rutile crystallites size and an increase of the amount of Mn–O–Ti bonds. The analysis based on the interpretation of both XRD patterns and FTIR spectrum allows one to explain the reduction of the crystallite size of rutile TiO<sub>2</sub> by an increase of the manganese loading.

## 1 Introduction

The titanium dioxide (TiO<sub>2</sub>) is an important multifunctional material due to its numerous applications, for example in solar cells, photo-catalyst devices, gas sensors, in various semiconductor devices (as a wide-bandgap n-type semiconductor), etc. It has three polymorphs, namely anatase, brookite, and rutile. Rutile is the most common and abundant stable phase of TiO<sub>2</sub> to which other phases transit when heated to a temperature above 600°C [1]. Rutile TiO<sub>2</sub> has many advantageous characteristics that are appropriate for various applications. For example, the high dielectric constant of rutile (close to 100) and high electric breakdown strength (> 100 kV/cm) make it a suitable dielectric material for high energy density capacitors [2]. The property of high refractive index has been used in both optical and anti-reflection coatings as well as in beam splitters [3]. The high thermal expansion of rutile is favorable for giving rise to a change in the semiconductor bandgap of dye-sensitized solar cells [4]. The surface properties of rutile such as the specific surface area, surface structure, active reaction sites are appropriate for uses in various photocatalytic processes [5,6] except the particle size of rutile, which is too large. This limits the utilization of such attractive and cost-effective material as a photocatalyst. All these facts and considerations motivated us to look for an alternative method to reduce

the particle size of rutile TiO<sub>2</sub>. One such way is to dope TiO<sub>2</sub> with metal ions.

Manganese ores can be used for doping TiO<sub>2</sub> due to their unique structures, uniform pores, and channels. In a previous study, Reddam et al., [7] have investigated the particles size and BET surface area of rutile of TiO<sub>2</sub>/manganese composite at 600°C. It has been found that the sizes of the rutile crystallites decrease from 41.35 to 31.01 nm for undoped TiO<sub>2</sub> and TiO<sub>2</sub>/manganese composite, respectively. Paul et al., [8] have prepared TiO<sub>2</sub>/manganese composite with 5 wt% manganese. The sizes of the rutile crystallites have been found to be 15 nm and 6 nm for undoped and manganese doped TiO<sub>2</sub>, respectively. In another study, Ettireddy et al., [9] have studied a TiO<sub>2</sub> supported manganese oxide catalysts and its specific surface area decreases from 54 to 49 m<sup>2</sup>/g when the content of SiO<sub>2</sub> increases from 2.5 wt% to 10 wt%. These studies have demonstrated that the manganese in TiO<sub>2</sub>/manganese could effectively limit the growth of crystallites. In the present work, we have studied the effects of the increased content of manganese and the temperature on the quantity of Mn-O-Ti bonds and their relationship to the size of the rutile crystallites.

## 2 Experimental Procedure

### 2.1 TiO<sub>2</sub> and Manganese composite preparation

The manganese ores were obtained from the artisanal mining area in Tasikmalaya, Indonesia. The materials for the samples were selected manually, cleaned by washing with water, and then dried in the sun. The dried manganese ores were crushed into small pieces with an area of approximately 1 cm<sup>2</sup>. Then, they were grinded using a jar mill to pass through a 150 mesh sieve. Table 1 shows the chemical composition of the prepared powder samples using crystalline TiO<sub>2</sub> powder and manganese ore. The sample of TiO<sub>2</sub>/manganese with a chemical composition of 20 wt% manganese (M20T) was prepared

**Table 1.** Chemical composition of samples of the synthesized TiO<sub>2</sub>-manganese composites

Sample	Manganese [g]	TiO <sub>2</sub> [g]
20 wt% Mn (M20T)	4	16
40 wt% Mn (M40T)	8	12
60 wt% Mn (M60T)	12	8
80 wt% Mn (M80T)	16	4

## 2.2 Sintering the synthesized TiO<sub>2</sub>-manganese composites

The powder samples were placed into a porcelain crucible and then inserted into a horizontal furnace, where they were sintered with a controlled heating rate of 10 °C/min up to the temperature of 1200 °C in air. Then the temperature was kept constant at 1200 °C for 2 hours. The cooling was performed by natural convection after turning off the electric furnace and leaving the samples inside.

## 2.3 Method for characterization of the synthesized TiO<sub>2</sub>-manganese composites

The experiments on the X-ray diffraction (XRD) of the samples have been carried out using a Smartlab X-ray diffractometer with filtered Cu K $\alpha$  radiation at a wavelength of 0.15418 nm. The accelerating voltage and the applied current were 40 kV and 30 mA, respectively. The diffraction patterns were registered over the range from 10° to 90° at a scan rate of 0.01 °/s. Fourier transform infrared (FTIR) spectra were obtained using a Varian 800 FTIR spectrometer (Scimitar Series model) in the wavenumber range of 400–4000 cm<sup>-1</sup> with a spectral resolution of 4 cm<sup>-1</sup>. All FTIR measurements were carried out at room temperature in a specular reflectance mode using the KBr pellet technique. The SEM images of fracture surface of samples were taken by using a scanning electron microscope (SEM) at a magnification of 1000-10,000 times and at accelerating voltage of 10-15 kV.

by dissolving 16 g of TiO<sub>2</sub> in a solution containing 50 mL ethanol and 50 mL deionized water, and then was stirred at 80 °C for one hour. Next, 4 g of the manganese ore powder was added slowly into the solution containing Ti<sup>2+</sup> ions under continuous stirring at 50 °C for 6 hours. The mixed solution was heated at 80 °C until the solvent completely evaporated. The resultant TiO<sub>2</sub>-manganese powder was dried in an oven at a temperature of 120 °C for 2 hours and then stored in a desiccator for a further treatment. The samples M40T, M60T and M80T were prepared following the same procedure.

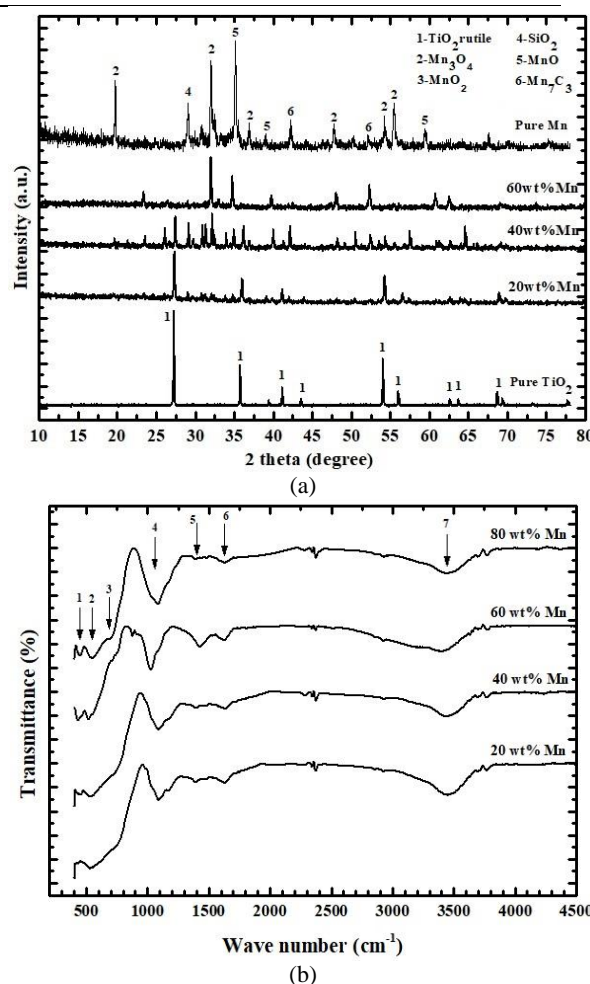


**Figure 1.** (a) XRD patterns and (b) FTIR spectra for TiO<sub>2</sub>/manganese composite with varying manganese content and sintered at 1200°C.

## 3 Results and Discussion

Figure 1a shows the XRD pattern of TiO<sub>2</sub>/manganese composite with a varying loading of manganese and sintered at 1200°C. In the sample of pure TiO<sub>2</sub>, some peaks appear at  $2\theta = 27.3^\circ, 35.8^\circ, 40.9^\circ, 44.5^\circ, 54.5^\circ, 56.3^\circ, 62.5^\circ, 63.6^\circ,$  and  $68.7^\circ$ . These peaks correspond to

the (110), (101), (111), (112), (211), (220), (002), (311), and (301) planes of the rutile  $\text{TiO}_2$  (R) (JCPDS 21-1276) [10]. This result is in agreement with the findings of the study of phase formation of  $\text{TiO}_2$  xerogel composites carried out by Aripin et al. [11, 12]. Then, for the sample of manganese ore (pure manganese), it consists of manganese oxide mainly in the form of pyrolusite ( $\text{MnO}_2$ ), quartz ( $\text{SiO}_2$ ), hausmannite ( $\text{Mn}_3\text{O}_4$ ), manganosite ( $\text{MnO}$ ), and manganese carbide ( $\text{Mn}_7\text{C}_3$ ). Hausmannite (peak 2) appears at  $2\theta = 18.31^\circ, 31.59^\circ, 36.29^\circ, 48.37^\circ, 54.78^\circ, \text{ and } 55.92^\circ$  (JCPDS 24-0734), manganosite (peak 5) at  $2\theta = 34.39^\circ, 36.69^\circ, \text{ and } 59.12^\circ$  (JCPDS 00-001-1206), and manganese carbide (peak 6) at  $2\theta = 41.47^\circ \text{ and } 51.18^\circ$  (PDF 01-075-1498). In the sample with 20 wt% Mn, the rutile  $\text{TiO}_2$  (peak 1) is formed as a major crystalline phase while quartz ( $\text{SiO}_2$ ) (peak 4), hausmannite ( $\text{Mn}_3\text{O}_4$ ) (peak 2) and manganosite ( $\text{MnO}$ ) (peak 5) as minor phases. As the loading increases, the peak intensity of rutile  $\text{TiO}_2$  decreases while the other crystalline phases tend to increase. With the increase of the loading up to 60 wt% Mn, crystalline rutile  $\text{TiO}_2$  gradually disappear. The crystallite size of the rutile phase has been evaluated using the Scherrer's equation [13] for the peak at  $2\theta = 27.3^\circ$ . The calculated size of rutile crystallites decreases from 70.81 nm to 27.18 nm, when the content of  $\text{TiO}_2$  increases from pure  $\text{TiO}_2$  to 60 wt% manganese. This means that the crystallite size of rutile can be correlated to the manganese content in the composite.

Figure 1b shows the FTIR spectra for  $\text{TiO}_2$ /manganese composite with varying manganese and sintered at  $1200^\circ\text{C}$ . For all samples, the band (peak 1) located at  $484.1 \text{ cm}^{-1}$  indicates the presence of  $\alpha\text{-Mn}_2\text{O}_3$  phase. The peak 2 that appears at  $533 \text{ cm}^{-1}$  corresponds to the Mn–O–Ti vibrational mode [7]. The peak 3 at  $696 \text{ cm}^{-1}$  can be assigned to Ti–O vibrational modes of rutile. The band (peak 4) identified at  $1020 \text{ cm}^{-1}$  can be attributed to pyrolusite ( $\text{MnO}_2$ ). These results are consistent with the XRD analysis reported above and are in quantitative agreement with the results reported in the literature for other  $\text{MnO}_2$  nanoparticles [14, 15]. The absorption bands (peak 5 and 6) observed at about  $1645$  and  $1386 \text{ cm}^{-1}$  were attributed to the bending H–O–H bond groups of adsorbed water molecules. The broad band (peak 6), at  $3452 \text{ cm}^{-1}$ , is attributed to the O–H stretching of hydroxyl groups that are present on the surface of the material [16]. It has been found that the integrated intensity of Mn–O–Ti bonds increases with increasing the amount of manganese ore. The high quantity of Mn–O–Ti bonds with smaller amounts of  $\text{TiO}_2$  indicates that more manganese ore particles facilitates the aggregation of  $\text{TiO}_2$ , and the manganese ores and  $\text{TiO}_2$  phases are not separated from each other in the composite. In this case, the presence of manganese ore particles impedes direct contact of  $\text{TiO}_2$  particles through Mn–O–Ti bonds, resulting in greater suppression of the phase transformation from anatase to rutile. Eventually, this leads to the formation of smaller particles of rutile  $\text{TiO}_2$  with smaller amounts of  $\text{TiO}_2$ .

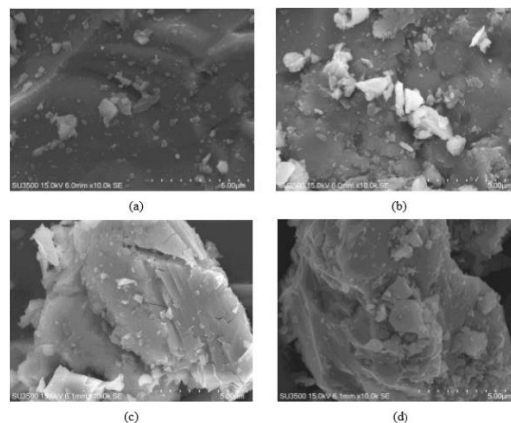


**Figure 2.** SEM images of  $\text{TiO}_2$ /manganese composite with (a) 20wt%Mn, (b) 40wt%Mn, (c) 60wt%Mn, and (d) 80 wt%Mn and sintered at  $1200^\circ\text{C}$ .

Figure 2 shows SEM images of  $\text{TiO}_2$ /manganese composite with a varying manganese content and sintered at  $1200^\circ\text{C}$ . The SEM image for samples of 20 wt% and 40 wt% illustrates that the micrographs are characterized by a dense grains with different texture and morphology and unevenly particle size distribution. The irregular-shaped grains with dark contrast are associated with the presence of  $\text{TiO}_2$ /manganese. The small grains of  $\text{SiO}_2$  with bright texture is dispersed on the surface of manganese. For samples with 60 wt% and 80 wt% of Mn, the microstructure of the samples includes large particles with an irregular shape. The larger particles, which can be seen in this figure are probably aggregates of the smaller particles, because based on the FTIR results for the case with a higher concentration of manganese, the presence of a big number of manganese particles facilitates the aggregation of  $\text{TiO}_2$ . It should be mentioned also that the manganese ores and the  $\text{TiO}_2$  phases are not separated from each other in the composite.

## 4 Conclusion

A novel  $\text{TiO}_2$ /manganese composite has been produced successfully from  $\text{TiO}_2$  and manganese ore by controlling the loading with manganese. The results presented in this paper show that an incorporation of manganese into  $\text{TiO}_2$  gives an appreciable effect on the crystallite size of  $\text{TiO}_2$  and on the formation of Mn–O–Ti bonds at a temperature of  $1200^\circ\text{C}$ . An interesting phenomenon has been observed analyzing the XRD pattern of the samples with a large loading with manganese. It has been found that the large amounts of manganese results in a significant decrease in the size of rutile crystallites. Such interpretation is supported by the observed large quantities of Mn–O–Ti bonds in  $\text{TiO}_2$ /manganese composite.

## Acknowledgments

This research was supported by a fund of the Siliwangi University through the Project of Research for Inovasi Perguruan Tinggi in 2017 with contract number: 1140/D3/PL/2017.

## References

1. A. Nilchi A, Janitabar-Darzi S, and Rasouli-Garmarodi S 2001 *Mater. Sci. Appl.* **2** 476.
2. Marinel S, Choi D.H, Heuguet R, Agrawal D, and Lanagan M 2013 *Ceram. Inter.* **39** 299.
3. Wang X, Wu G, Zhou B, and Shen J. *Mater.* **6** 2819.
4. Alivov Y and Fan Z.Y 2009 *Appl. Phys. Lett.* **95** 16.
5. Mahltig B, Haufe H, Kim C,W, Kang Y. S, Gutmann E, Leisegang T, and Meyer D.C 2013 *Croat. Chem.Acta* **86** 143.
6. Jin Q, Arimoto H, Fujishima M and Tada T *Catal.* **3** 444.
7. Abdelouahab-Reddam H, Abdelouahab-Reddam Z, El Mail R, and Aaliti A 2014 *Intern. J. Innov. Appl. Stud.* **8** 660.
8. Paul S, and Choudhury A 2012 *Intern. J. Inov. Res. Develop.* **1** 24.
9. Ettireddy P, Ettireddy N, Mamedov S, Boolchand P, Smirniotis P 2007 *Appl. Catal. B Environ.*, **76** 123.
10. JCPDS-International Centre for Diffraction Data, 1997 PCPDFWIN **1.30**.
11. Aripin H, Joni I.M, Mitsudo S, Sudiana I.N, Priatna E, Busaeri N, and Sabchevski S 2017 *Intern. J. Techn.* **8** 1507.
12. Aripin A, Mitsudo S, Sudiana I.N, Busaeri N, Sunendar B, Sabchevski S 2016 *Mater. Sci. Forum* **872** 81.
13. Duy P.P, Kim K.K, Cao V.T, Van Q.V, and Thi T.V 2014 *Intern. J Mater. Sci. Appl.*, **3** 147.
14. Yang X.J, Liu Z, Makita M, and Ooi K 2004 *Chem. Mater.* **16** 5581.
15. Yang R, Wang Z, Dai L, and Chen L 2005 *Mater. Chem. Phys.* **93** 149.
16. Yang S and Gao L 2006 *J. Amer. Ceram. Soc.* **89** 1742.